THE JOURNAL OF BIOLOGICAL CHEMISTRY VOL. 284, NO. 1, pp. 284–291, January 2, 2009

Crystal Structures of the Lyn Protein Tyrosine Kinase Domain in Its Apo- and Inhibitor-bound State*

Received for publication, October 10, 2008 Published, JBC Papers in Press, November 4, 2008, DOI 10.1074/jbc.M807850200

Neal K. Williams[‡], Isabelle S. Lucet[‡], S. Peter Klinken[§], Evan Ingley[§¶], and Jamie Rossjohn[‡1]

From the [‡]Protein Crystallography Unit, Department of Biochemistry and Molecular Biology, School of Biomedical Sciences, Monash University, Clayton, Victoria 3800, Australia, and the [§]Laboratory for Cancer Medicine and [¶]Cell Signalling Group, Western Australian Institute for Medical Research and Centre for Medical Research, The University of Western Australia, Perth, Western Australia 6000, Australia

The Src-family protein-tyrosine kinase (PTK) Lyn is the most important Src-family kinase in B cells, having both inhibitory and stimulatory activity that is dependent on the receptor, ligand, and developmental context of the B cell. An important role for Lyn has been reported in acute myeloid leukemia and chronic myeloid leukemia, as well as certain solid tumors. Although several Src-family inhibitors are available, the development of Lyn-specific inhibitors, or inhibitors with reduced off-target activity to Lyn, has been hampered by the lack of structural data on the Lyn kinase. Here we report the crystal structure of the non-liganded form of Lyn kinase domain, as well as in complex with three different inhibitors: the ATP analogue AMP-PNP; the pan Src kinase inhibitor PP2; and the BCR-Abl/Src-family inhibitor Dasatinib. The Lyn kinase domain was determined in its "active" conformation, but in the unphosphorylated state. All three inhibitors are bound at the ATP-binding site, with PP2 and Dasatinib extending into a hydrophobic pocket deep in the substrate cleft, thereby providing a basis for the Src-specific inhibition. Analysis of sequence and structural differences around the active site region of the Src-family PTKs were evident. Accordingly, our data provide valuable information for the further development of therapeutics targeting Lyn and the important Src-family of kinases.

Lyn is a member of the Src family of intracellular membrane-associated tyrosine kinases. While the N terminus of each member is unique, this family shares significant homology in the kinase domain, as well as the SH2/SH3 protein interaction domains. Tyrosine phosphorylation controls the activity of Lyn, and other Src family kinases, in two opposing ways (1, 2). Phosphorylation of the C-terminal tail ($pTyr^{508}$ in Lyn) inhibits activity through promoting its association with the kinases own SH2 domain. In contrast, phosphorylation of a residue within the activation loop ($pTyr^{397}$) results in activation of the enzyme. Enzymatic inhibition is also enhanced by the binding of the kinases SH3 domain to a left-handed polyproline type II helix situated between the SH2 and kinase domains (2). The SH2 and SH3 domains are also utilized by the enzyme for its activation, as well as inactivation, through specific interactions with proteins containing polyproline and/or phosphotyrosine motifs, thus also allowing specific targeting of the kinases to specific substrates/subcellular compartments (3).

The involvement of Src family kinases in various signaling cascades including cytokine receptor pathways (4, 5) is gradually being elucidated (6). Lyn is expressed in hemopoietic cells of erythroid/myeloid and B lymphoid origin (7–9), neuronal cells, prostate cells (10), colon cells (11), and is involved in the transmission of signals from a number of receptors such as Epo (7, 12, 13), c-Kit (14), B cell antigen, and c-Mpl (15) receptors (4). Lyn phosphorylates a number of signaling molecules, including PI 3-kinase, PLCγ2, HS1 (16), Cbp (17), STAT5 (18), and MAP kinase, and $Lyn^{-/-}$ mice display severe defects in the immune system (19) and the erythroid compartment (13, 20).

An important role for Lyn in leukemia has been suggested by several studies (21–25). Primary acute myeloid leukemia (AML) cells display elevated Lyn kinase activity (21) and Lyn is critical for maintaining AML cell proliferation and anti-apoptotic pathways (26). While the BCR-Abl fusion protein is the initiating molecule for chromic myeloid leukemia (CML), there is a crucial downstream role for Lyn in BCR-Abl-induced leukemogenesis (23–25). There is a direct link between Lyn and BCR-Abl signaling pathways as Lyn phosphorylates Tyr^{177} of BCR-Abl (27, 28), thus recruiting the adaptor Gab2, both of which are essential for BCR-Abl oncogenesis (29). Significantly, Imatinib-resistant CML cells have elevated Lyn levels and kinase activity (22). Further, ablation of Lyn from Imatinib-resistant CML cells resulted in the induction of apoptosis (30).

A significant role for Lyn in the development of certain solid tumors has also come to light. Colon carcinoma cells utilize Lyn in the activation of the Akt anti-apoptotic pathway, and drug-resistant cells show elevated Lyn kinase activity (11). Lyn is also involved in the signaling mechanisms regulating prostate cancer cells (31). Significantly, inhibition of Lyn in prostate cancer cell lines resulted in reduced proliferation *in vitro* and in prostatic cancer xenograft models (10). Thus several lines of evi-

* This work was supported by grants from the National Health and Medical Research Council (NHMRC) of Australia (303101, 403987, and 513714), the Medical Research Foundation of Royal Perth Hospital, and the Centre for Food and Genomic Medicine and by a NHMRC Industry Fellowship (to N. K. W.) and ARC Federation Fellowship (to J. R.). The costs of publication of this article were defrayed in part by the payment of page charges. This article must therefore be hereby marked "*advertisement*" in accordance with 18 U.S.C. Section 1734 solely to indicate this fact.

The atomic coordinates and structure factors (codes 2ZV7, 2ZV8, 2ZV9, and 2ZVA) have been deposited in the Protein Data Bank, Research Collaboratory for Structural Bioinformatics, Rutgers University, New Brunswick, NJ (http://www.rcsb.org/).

[1] To whom correspondence should be addressed: Protein Crystallography Unit, Dept. of Biochemistry and Molecular Biology, Monash University, Clayton, VIC 3800, Australia. Tel.: 61-3-9905-3736; Fax: 61-3-9905-4699; E-mail: jamie.rossjohn@med.monash.edu.au.

dence point to a significant involvement of Lyn in both leukemic and solid tumor development.

The Src-family as well as other cytoplasmic (*e.g.* Abl) and receptor (*e.g.* EGF-R) tyrosine kinases are important targets or therapeutic intervention (32, 33). Several specific (*e.g.* Imatinib) and some less specific (*e.g.* Dasatinib) small molecules have been generated that mostly act as ATP competitive inhibitors and have been successfully employed for leukemia/cancer treatment in the clinic (32, 33). Crystal structures of Src (1, 34), Hck (35, 36), and Lck (37, 38) have enabled a detailed investigation of how the Src family of kinases are regulated, and the way in which small molecule inhibitors can inactivate these enzymes. To extend our understanding, and provide a structural framework for the design of specific inhibitors to the Src family of kinases, we have determined the crystal structures of the kinase domain of Lyn in complex with 3 different inhibitors, AMP-PNP,[2] PP2, and Dasatinib, as well as the non-liganded form of the enzyme, at 2.5–2.7-Å resolution.

EXPERIMENTAL PROCEDURES

Plasmid Construction—All plasmid constructs were generated by site-directed mutagenesis using oligonucleotides and subcloned in-frame into the appropriate vector and confirmed by sequencing. The murine Lyn kinase domain (amino acids 239–512) was subcloned in to the baculovirus expression vector pFastBacHTA (Invitrogen) generating a His_6-tagged fusion resulting in a 5-amino acid N-terminal extension (GAMDP) to the Lyn kinase domain after tobacco etch virus (TEV) cleavage. The murine Csk-binding protein (Cbp, amino acids 74–474) was subcloned into pET44a (Merck, Darmstadt, Germany) to be expressed as a NusA-His_6-tagged fusion in bacteria (Rosetta2, Merck), with replacement of the thrombin with a TEV cleave site using site-directed mutagenesis, for expression and purification using the Profinia system (Bio-Rad) for use as a biologically significant substrate for Lyn kinase assays.

Protein Expression and Purification of Lyn Kinase Domain—Recombinant bacmid DNA was isolated and used to transfect *Spodoptera frugiperda* (Sf9) insect cells. Baculovirus obtained from the transfection culture was used to infect Sf9 cells grown in suspension to a density of 2×10^6 cells per ml, at a multiplicity of infection greater than 10, and harvested 48 h after infection. Cells were resuspended in a buffer consisting of 20 mM Tris HCl, pH 8.0, 500 mM NaCl, 5% glycerol, 3 mM β-mercaptoethanol, 0.1% thesit, supplemented with complete protease inhibitors mixture (Roche Applied Sciences), lysed by sonication and centrifuged at 45,000 $\times$ *g* for 1 h at 4 °C. The supernatant was filtered and loaded onto ProBond nickel-chelating resin (Invitrogen). After extensive washing, the recombinant protein was eluted with buffer plus 100–300 mM imidazole and Lyn-containing fractions were pooled. The His_6 tag was removed by treatment with TEV protease during overnight dialysis against 20 mM Tris HCl, pH 8.0, 25 mM NaCl, 5% glycerol, 2 mM DTT, 0.5 mM EDTA, at 4 °C. The digested protein was bound to a HiTrap Q column (GE Healthcare) equilibrated in the same buffer and eluted with a NaCl gradient. Lyn-containing fractions were pooled, concentrated to 2.5 ml and loaded onto a Superdex 75 gel filtration column (HiLoad 16/60; GE Healthcare) equilibrated in 20 mM Tris-HCl, pH 8.0, 200 mM NaCl, 2 mM DTT, 0.5 mM EDTA. Purified Lyn kinase domain was concentrated to 8 mg/ml for crystallization.

Protein Analysis and Western Blotting—Mass spectrometric analysis of purified Lyn protein before and after auto-kinase assays were performed by Proteomics International (East Perth, WA, Australia) on protein gel plugs that were destained, trypsin-digested, and peptides extracted according to standard techniques (39). Peptides were analyzed by electrospray ionization mass spectrometry (LC/MS) using the Ultimate 3000 HPLC system (Dionex, Sunnyvale, CA) coupled to a Q TRAP 4000 mass spectrometer (Applied Biosystems, Foster City, CA). Tryptic peptides were loaded onto a C18PepMap100 reversed phase column (Dionex) and separated with a linear gradient of water/acetonitrile/0.1% formic acid (v/v) at a flow rate of 300 nl/min. Spectra were analyzed to identify proteins of interest using Mascot sequence matching software (Matrix Science, London, UK) with the data base and taxonomy set as Ludwig NR and All Taxonomy, respectively. The phosphorylation detection was achieved with precursor ion scanning for a loss of 79 mass units in negative mode (PO_3^-) and subsequent MSMS fragmentation of those selected peptides to determine their identity. Protein concentration was estimated using the Bio-Rad D_c protein assay according to the manufacturer's instructions, using bovine serum albumin as a standard.

Exo-kinase kinase assays were performed essentially as previously described (7), with minor modifications, using NusA-Cbp (5 mg/ml) as substrate in 50 mM Tris-HCl, pH 7.4, 1 mM DTT, 10 mM $MgCl_2$, 50 μM ATP, at 30 °C. Kinase inhibitors Dasatinib (Bristol-Myers-Squibb, New York, NY), PP2 (Merck) and SU6656 (Merck) were added to reaction mixtures 10 min prior to the addition of ATP. Auto-kinase reactions were undertaken under identical conditions to those described for the exo-kinase assays, only no NusA-Cbp substrate was added. Reactions contained 0.1 μg/10 μl Lyn kinase and were stopped by the addition of SDS loading buffer. Reactions were then analyzed by Western blotting for phosphotyrosine incorporation into the Cbp substrate.

Western blotting was performed essentially as described previously (7, 40). Antibodies used included anti-phosphotyrosine 4G10-HRP (Millipore, Billerica, MA) and anti-phospho-Src (pY^{416}) (Cell Signaling Technology, Danvers, MA). Secondary antibodies were coupled to horseradish peroxidase (Amersham, Buckinghamshire, UK) and detected by enhanced chemiluminescence (Amersham Biosciences). Western blots were quantitated using a ChemDoc XRS (Bio-Rad) and Quantity One (v4.5.2, Bio-Rad).

Crystallization of Lyn Kinase Domain and Formation of Inhibitor Complexes—Crystals were grown at 4 °C using the hanging-drop vapor-diffusion method. Purified Lyn kinase domain was mixed with an equal volume of a reservoir solution containing 23% polyethylene glycol 3350, 0.1 M NaCl, and 0.1 M Na.Hepes, pH 7.5. Crystals formed after 1–3 days. Inhibitors PP2 (1-tert-butyl-3-(4-chlorophenyl)-2H-pyrazolo[4, 5-e]pyrimidin-1-ium-4-amine) and Dasatinib (BMS-354825; *N*-(2-chloro-6-methylphenyl)-2-(6-(4-(2-hydroxyethyl)piperazin-1-

[2] The abbreviations used are: AMP-PNP, adenosine 5′-(β,γ-imino)triphosphate; PTK, protein-tyrosine kinase domain; VDW, van der Waals; DTT, dithiothreitol; r.m.s.d., root mean square deviation.

TABLE 1
Data collection and refinement statistics

	Apo-Lyn	Lyn-PP2	Lyn-Dasatinib	Lyn-AMP-PNP
Temperature	100K	100K	100K	100K
Space group	H3	H3	H3	H3
Cell dimensions (Å) (a = b, c)	127.31, 53.84	128.47, 54.17	127.38, 55.62	127.24, 54.88
Resolution limits (Å)[a]	63.3-2.5 (2.64-2.5)	48.7-2.76 (2.91-2.76)	39.2-2.6 (2.74-2.6)	38.9-2.7 (2.85-2.7)
No. observations	28576	16674	24621	18056
No. unique reflections	11259	8337	10106	9082
Completeness (%)[a]	100 (100)	97.1 (83.0)	97.6 (95.7)	99.8 (100)
R_{merge} (%)[a,b]	3.7 (35.3)	4.3 (33.8)	5.4 (35.4)	4.3 (34.1)
$I/\sigma I$[a]	21.1 (2.2)	16.3 (2.0)	16.6 (2.3)	17.1 (2.1)
Multiplicity	2.5	2.0	2.4	2.0
R-factor (%)[c]	20.5	19.5	19.8	19.9
R-free (%)[c]	23.8	23.1	23.1	24.5
Number of atoms:				
-Protein	2044	2031	2081	2044
-Ligand	21	33	31	
-Water	14	16	38	15
Ramachandran plot, most favored %	94	90	95	94
R.m.s.d. from ideality				
Bond lengths (Å)	0.007	0.008	0.007	0.011
Bond angles	1.035	1.235	1.204	1.153

[a] The value in parentheses is for the highest resolution bin (approximate interval, 0.1 Å).
[b] $R_{merge} = \Sigma|I_{hkl}-<I_{hkl}>|/\Sigma I_{hkl}$.
[c] $R_{factor} = \Sigma I_{hkl}½|F_o - |F_c½½|/\Sigma I_{hkl}|F_o|$ for all data except 5%, which was used for the R_{free} calculation.

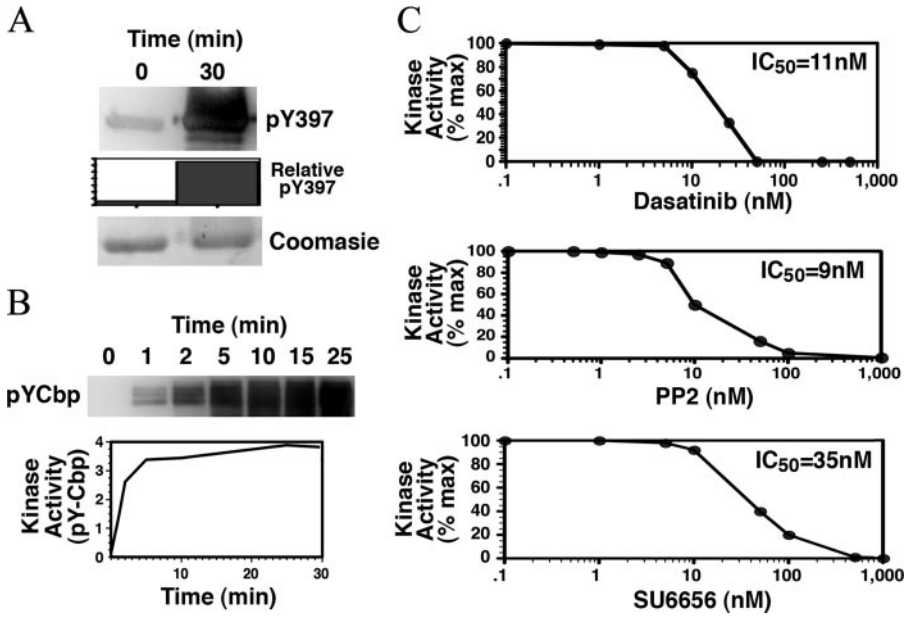

FIGURE 1. **Biochemical analysis of the purified Lyn kinase domain.** *A*, Lyn auto-phosphorylates its activation loop. Purified Lyn kinase domain was analyzed for phosphorylation of Tyr^{397} using the Src pY^{416}-specific antibody. Phosphorylation of Tyr^{397} detected by Western blotting was quantitated relative to total protein using Quantity One (Bio-Rad). *B*, exo-kinase activity of Lyn. Analysis of the Lyn kinase domains ability to phosphorylate Cbp. Western blots using anti-pY-HRP coupled antibodies were quantitated as in *A* above. *C*, determination of IC_{50} values for Dasatinib, PP2, and SU6656 for the Lyn kinase domain. Kinase assays were performed using Cbp as a substrate with various concentrations of inhibitors (Dasatinib, PP2, SU6656) and Western blots of phospho-Cbp analyzed as in *A* above.

yl)-2-methylpyrimidin-4-ylamino)thiazole-5-carboxamide) in DMSO at 10 mM, or diluted 10-fold in reservoir solution, were added to drops containing Lyn crystals, and incubated at 4 °C for 1–2 h. AMP-PNP and $MgCl_2$ at 50 mM each were added to crystal-containing drops and incubated for up to 3 weeks at 4 °C.

X-Ray Data Collection, Structure Determination, and Refinement—Crystals were flash-frozen using the reservoir solution plus 10% glycerol as a cryoprotectant. Data sets at 2.5–2.76-Å resolution were merged and processed using MOSFLM and SCALA in the CCP4i suite. The crystals, with unit cell dimensions $a = b = 127.3$ Å and $c = 53.8$ Å, belong to space group H3, with one monomer in the asymmetric unit. The apo-structure was solved by molecular replacement using the program PHASER in the CCP4i suite. Lck was used as a search model (Protein Data Bank ID: 1QPD) with all non-conserved residues substituted with alanine. The structure was refined using the CCP4i suite program REFMAC5 by rigid body fitting followed by restrained refinement interspersed with rounds of model building with the program COOT.

For inhibitor complex structures, difference Fourier analyses were used to evaluate ligand binding. Accordingly, unbiased features in electron density maps revealed the location of inhibitor molecules, and the subsequent structures were refined as listed above. For refinement of the inhibitor complexes, the same R_{free} data set as selected in the apo crystal form. A summary of the data collection and refinement statistics is presented in Table 1.

RESULTS AND DISCUSSION

Biochemical Analysis of Purified Lyn Kinase Domain—The purified kinase domain of Lyn was assessed for post-translational modifications by Western blot and mass spectrometry analysis. Using an antibody specific for the common activation loop phosphorylation site found in Src family kinases ($pTyr^{416}$

in Src, pTyr^{397} in Lyn), only after auto-activation was significant reactivity observed (Fig. 1*A*). This was confirmed by mass spectrometric analysis, showing the purified kinase domain was essentially unphosphorylated at this site, but upon incubation with Mg^{2+}-ATP it became rapidly phosphorylated. The enzyme was also able to rapidly phosphorylate the substrate Cbp in exo-kinase assays showing the capacity of the purified protein to display functional activity (Fig. 1*B*). Further, the ability of small molecules to inhibit the enzymes ability to phosphorylate Cbp were analyzed, showing Dasatinib (IC_{50} 11 nM), PP2 (IC_{50} 9 nM), and SU6656 (IC_{50} 35 nM) could all strongly inhibit the activity of Lyn (Fig. 1*C*). The PP2 and Dasatinib inhibitors were then used to examine the structural basis of binding and specificity by x-ray crystallography.

Structure of the Lyn Kinase Domain—To determine the overall atomic architecture of the Lyn PTK, and provide a baseline for structural comparison of inhibitor binding to Lyn, the kinase domain of murine Lyn was crystallized in the absence of inhibitor and its structure determined at 2.5-Å resolution and refined to an R_{fact} = 20.5% and R_{free} = 23.8%. The refined model, comprising residues 239–501, is typical of the bi-lobal protein-tyrosine kinase fold and closely resembles the structures of Src, Lck, and Hck (Fig. 2*A*). Briefly, the N-terminal lobe of the PTK consists of a 5-stranded anti-parallel twisted β-sheet and a single large α-helix, termed the αC helix. The C-terminal lobe is larger and predominantly helical, but includes a 2-stranded anti-parallel β-sheet. Between the two lobes is a deep cleft that forms the ATP-binding pocket, and connecting them is a loop that borders the cleft and forms a hinge that confers flexibility to the overall structure, allowing for relative movement of the lobes.

The catalytic activity of protein tyrosine kinase can be regulated by the phosphorylation state of the activation loop Tyr residue (Tyr^{397} in Lyn) and is correlated with movements in the loop and αC. The region of the activation loop spanning this residue is thus highly flexible, and in the apo Lyn structure residues 393–399, inclusive, are disordered and not included in the model, thus not revealing the phosphorylation state of Tyr^{397}, although Western blot and mass spectrometric analyses clearly indicated that the Lyn PTK was unphosphorylated. Structural comparison with unphosphorylated, inactive Src and Hck, and active, phosphorylated Lck (Fig. 2*B*) shows that despite the lack of phosphorylation in Lyn PTK, the activation loop and αC are in the active conformations.

AMP-PNP Binding to Lyn—To provide a model for the substrate-bound state of the enzyme, Lyn crystals were soaked with the non-hydrolyzable ATP analogue adenyl imidodiphosphate (AMP-PNP) in the presence of Mg^{2+} ions and the resulting complex was solved at 2.7 Å resolution and refined to an R_{fact} = 19.9% and R_{free} = 24.5%. As expected, AMP-PNP binds in the cleft between the two lobes of the kinase domain (Fig. 3*A* forming extensive van der Waals (VDW) and hydrogen-bonding interactions. The planar adenine ring is sandwiched between the hydrophobic residues of the N-terminal lobe (Leu^{253}, Val^{261}, and Ala^{273}), the hinge region (Phe^{321} and Met^{322}) and the C-terminal lobe (Leu^{374}). In addition, two hydrogen bonds link the adenine group through N^6 and N^1 to the hinge residues Glu^{320O} and Met^{322N}, respectively, as seen with AMP-PNP-

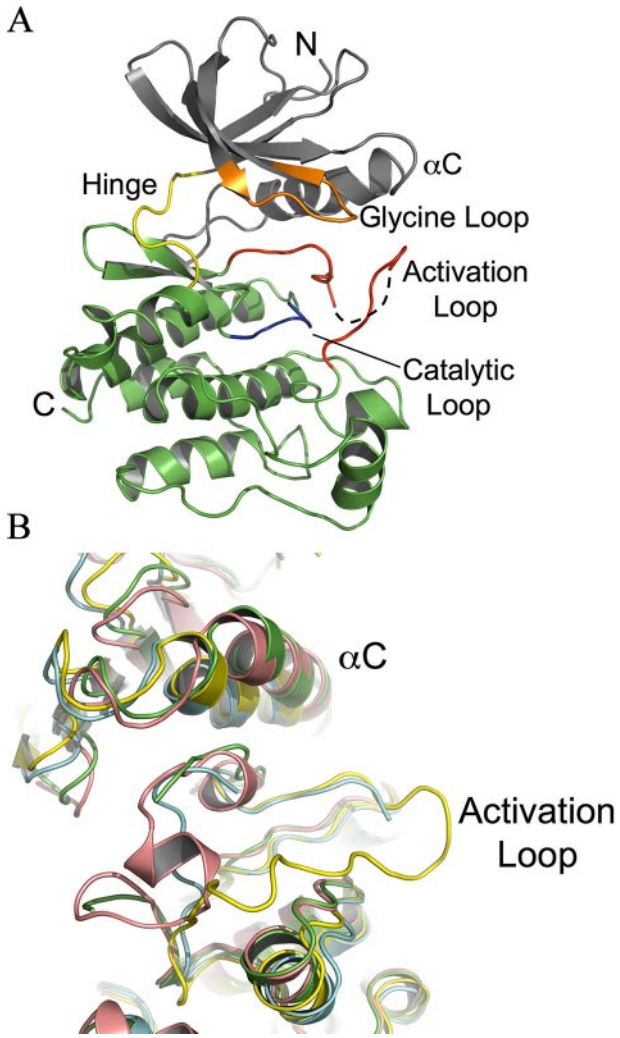

FIGURE 2. **Overview of the crystal structure of Lyn.** *A*, ribbon representation of the crystal structure of Lyn PTK. The N-terminal lobe (residues 239–326) shown in gray comprises a five-stranded anti-parallel β-sheet and one α-helix (αC). The C-terminal lobe (residues 327–501) is shown in *green*. The glycine loop is colored in *orange*, the hinge region between the two lobes in *yellow*, the catalytic loop in *blue*, and the activation loop in *red*. *B*, close-up of portions of the αC helix and activation loop showing active (Lyn (blue), Lck (yellow)) and inactive (Src (magenta), Hck (green)) conformations.

binding to other Src family kinases. In the published complexes of AMP-PNP with Src (1) and Lck (38), the ribose group is hydrogen-bonded to the Ser residue conserved in all but one Src-family PTKs (326 in Lyn) either through a water-mediated hydrogen bond in Src, or directly in the case of Lck where the side chain points toward the ligand. In the Lyn structure, as in Src, Ser^{326} is pointing away from the ribose group, but at the resolution of this Lyn structure, no hydrogen-bonded water molecule is detected. Asp^{385} of the conserved DFG motif forms hydrogen bonds with the α- and β-phosphates and a water-mediated hydrogen bond to the imido-nitrogen. The β-phosphate group interacts with the glycine loop residues Ala^{255} and Gly^{259} via a water molecule that is accommodated by a small shift in the loop location with respect to the apo structure. A third water molecule links Arg^{369} to the γ-phosphate. Thus, extensive contacts and hydrogen bonds anchor the substrate analogue and poise the tri-phosphate group for catalysis.

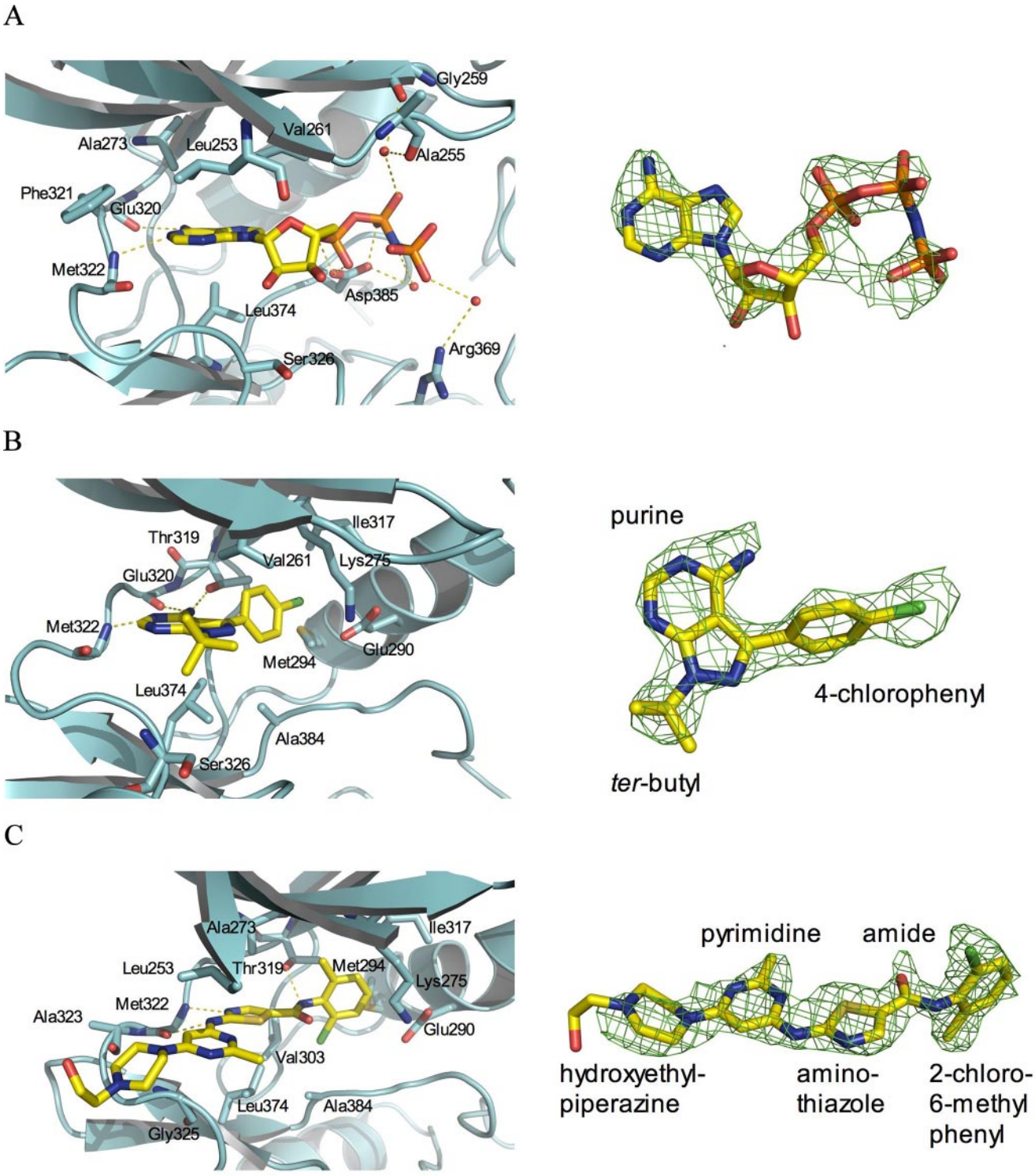

FIGURE 3. **Mode of inhibitors binding to Lyn PTK.** *A*, interaction between AMP-PNP and Lyn PTK. *B*, interaction between PP2 and Lyn PTK. *C*, interaction between Dasatinib and Lyn PTK. *Left panel*, the side chains of residues that interact with the inhibitor are shown, as are main-chain atoms and water molecules participating in hydrogen bonds. *Right panel*, corresponding view of the inhibitor in a *ball-and-stick* representation and covered with the simulated annealing omit-map Fo-Fc electron density map contoured at 2σ.

PP2 Binding to Lyn—For insight into the structural basis of small molecule inhibition of Lyn PTK by the pan-Src kinase inhibitor PP2, the PP2-Lyn complex was formed by soaking apo Lyn crystals with PP2, and the structure was solved at 2.76-Å resolution and refined to an R_{fact} = 19.5% and R_{free} = 23.1% (Fig. 3*B*). PP2 binds to Lyn kinase in a very similar position to AMP-PNP, with the respective purine rings almost co-planar. The two adenine group hydrogen bonds to residues Glu^{320} and Met^{322} are present, with a third, absent in the AMP-PNP structure, between N25 of the inhibitor and Thr^{319OG}. This hydrogen bond, seen in PP2 binding to Lck (38) and the closely related inhibitor PP1 binding to Hck (36), is made possible by the

purine group of PP2 inserting slightly more deeply into the nucleotide-binding cleft than in AMP-PNP, and a concomitant movement of Thr^{319} to accommodate the chlorophenyl moiety of the inhibitor. The chlorophenyl ring is rotated some 67° with respect to the plane of the purine ring system and buried in a hydrophobic pocket not occupied by ATP, having VDW interactions with Lys^{275}, Glu^{290}, Met^{294}, Ile^{317}, Thr^{319}, and Ala^{384}. The *ter*-butyl substituent extends toward the ribose-binding pocket and makes VDW contacts with Val^{261}, Ser^{326}, and Leu^{374}.

Dasatinib Binding to Lyn—Dasatinib is a multi-target kinase inhibitor recently approved for treatment of chronic myeloid leukemia, and showing promise in the treatment of several solid tumors. For further insight into the structural basis of specific inhibitor binding, Lyn crystals were soaked with Dasatinib and the resulting complex structure solved to 2.6-Å resolution and refined to an $R_{fact} = 19.8\%$ and $R_{free} = 23.1\%$ (Fig. 3*C*). The deep hydrophobic pocket that accommodates the chlorophenyl moiety of PP2 here is occupied by the 2-chloro-6-methyl phenyl group of Dasatinib, which makes extensive VDW contacts with Lys^{275}, Glu^{290}, Met^{294}, Val^{303}, Ile^{317}, Thr^{319}, and Ala^{384}. The aminothiazole ring of Dasatinib is located approximately where the purine ring of PP2 is situated, participating in a hydrogen bond to Met^{322N} through the ring nitrogen, and having VDW contacts with Ala^{273} and Leu^{374}. Two other hydrogen bonds are also present, between Thr^{319OG} and the amide nitrogen of Dasatinib, and Met^{322O} with the amino group. The pyrimidine ring extends out of the binding pocket through a cleft formed by Leu^{253} and Gly^{325}, with the hydroxyethyl-piperazine group largely solvent-exposed but making VDW contact with Ala^{323}. The crystal structure of Dasatinib bound to Abl kinase domain has recently been reported (41) and the binding mode seen is very similar to that found here with Lyn. The hydrogen bonds identified in the Lyn complex are present in the Abl structure including with the counterpart of Thr^{319} that is conserved among the Src-family as well as the closely related Abl kinase.

Comparison of Inhibitor Binding to Lyn and Related Structures—The binding of the three structurally distinct inhibitors to Lyn caused only minor changes in the overall structure from the unliganded state, with root mean square (r.m.s.) deviations upon binding of 0.274 Å over 244 Cα atoms for AMP-PNP, 0.246 Å over 235 Cα atoms for PP2, and 0.396 Å over Cα atoms for Dasatinib (Fig. 4). Comparison of these Lyn structures with related PTKs similarly reveals a high degree of structural conservation. Given the high degree of sequence identity among the Src-family of PTKs (Fig. 5*A*) this structural conservation is not surprising and highlights the significant challenge faced in designing inhibitors specific to individual members.

AMP-PNP binding is expected to closely mimic that of substrate ATP. The Lyn-AMP-PNP structure reveals 2 hydrogen bonds to main chain atoms of highly conserved residues in PTKs and phosphate interactions with catalytic residues as well as conserved regions of the glycine loop. By contrast, PP2 exerts Src-family selectivity through a unique hydrogen bond to Thr^{319}, a residue conserved among this group of kinases (Fig. 5*A*). Furthermore, the chlorophenyl moiety is positioned within a hydrophobic pocket, access to which is made possible

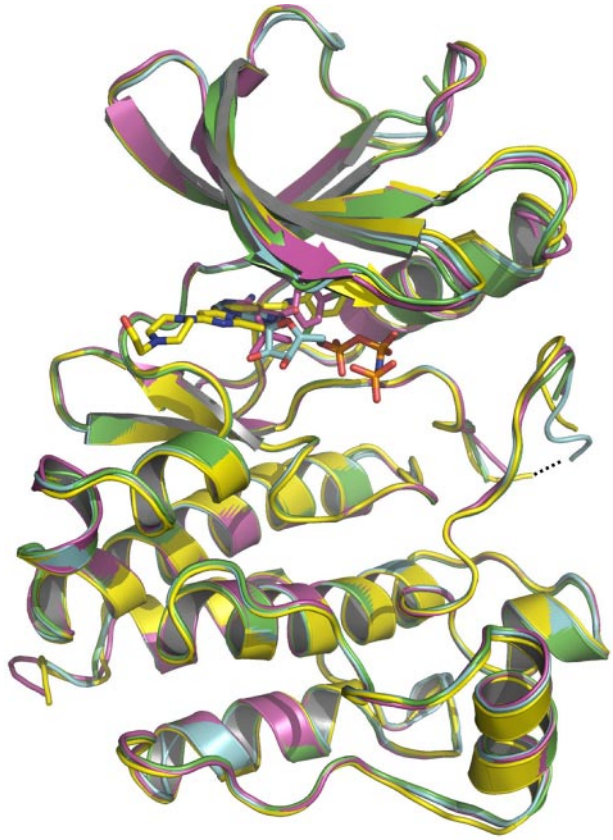

FIGURE 4. **Superimposition of apo-Lyn and Lyn-inhibitor complexes.** Apo-Lyn (*green*), Lyn-AMP-PNP (*blue*), Lyn-PP2 (*magenta*), Lyn-Dasatinib (*yellow*). Inhibitors are shown in *ball-and-stick* representation.

by Thr^{319} substituting the gate-keeper Met residue conserved in many PTKs (38). Superimposing the Lyn-PP2 complex with the published Lck-PP2 structure (Fig. 5*B*) reveals a small r.m.s. deviation of 0.686 Å over 230 Cα atoms. Only 2 amino acid substitutions between Lyn and Lck exist around the active site. The hinge residues Ala^{323} and Lys^{324} of Lyn correspond to Lck Glu^{320} and Asn^{321}. Indeed, these sequence positions are the most variable around the active site of the Src-family kinases. The main chain atoms of these residues are superposable in the two structures, and the small size of PP2 means that the side chains of neither residue are contacted by the molecule, consistent with PP2 being a pan-Src family inhibitor. Nonetheless, the amino acid substitutions at these positions may present exploitable differences in the future design of more selective inhibitors.

Dasatinib was originally designed as a selective inhibitor to the Src kinases (42) and subsequently identified as a useful BCR-Abl inhibitor (43). Dasatinib is able to inhibit forms of BCR-Abl harboring point mutations that confer resistance to Gleevec (Imatinib) and arise during drug treatment. This results from Dasatinib binding to the active state of the kinase rather than being limited to the inactive state in the case of Gleevec (44). The Lyn-Dasatinib complex determined here is the first reported structure of this inhibitor with an Src-family PTK. The specificity of Dasatinib is exerted through similar active site interactions to those of PP2. Structural alignment of the Lyn-Dasatinib complex with the Abl complex (41) gives an

A

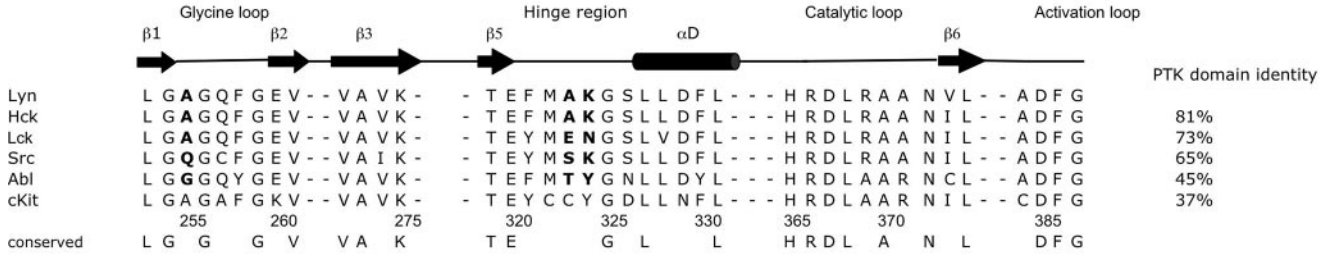

B

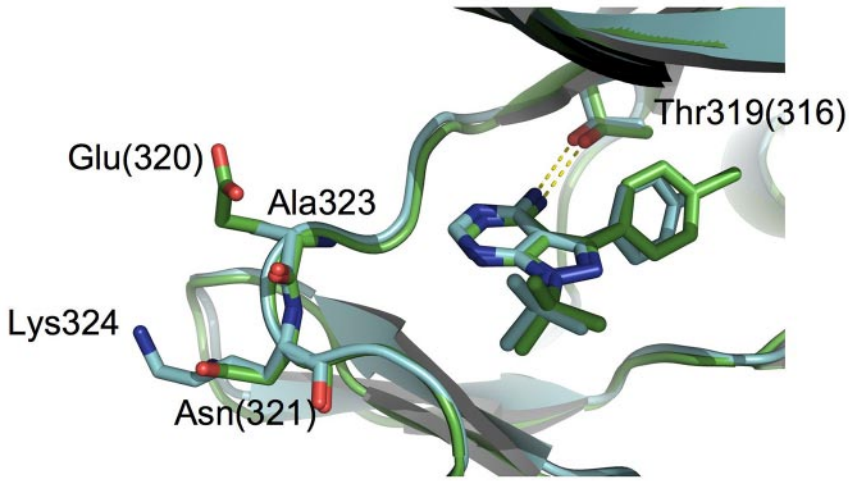

C

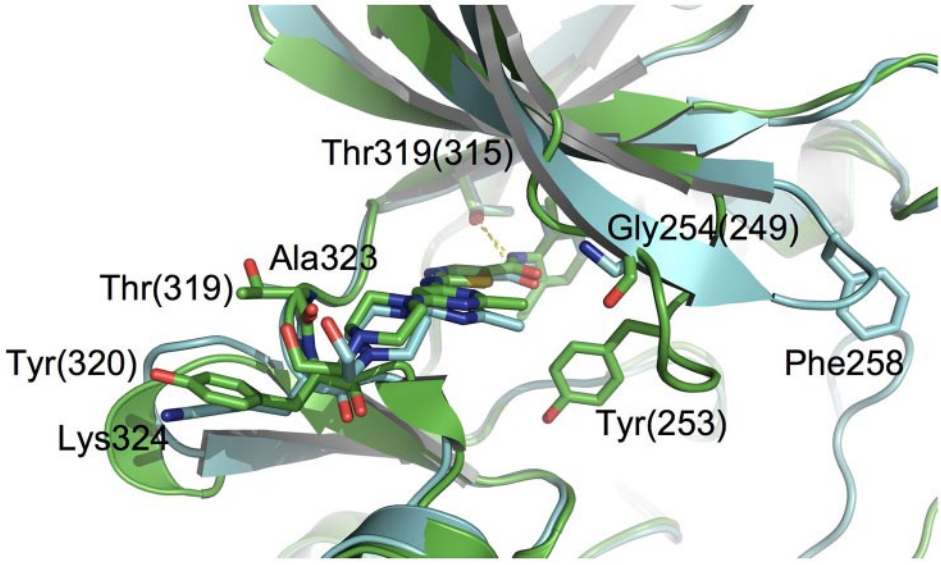

FIGURE 5. **Comparison of the active site region of Lyn with other PTKs.** *A*, amino acid sequence alignment of the ATP binding site region of human Lyn PTK domain with the other members of the Src-family, as well as cKit. Variable residues are indicated in *bold face*. Sequence identity of Lyn with each kinase is indicated on the *right*. *B*, superimposition of Lyn- (*blue*) and Lck- (1QPE; *green*) PP2-binding sites. Lck residues numbers are in *parentheses*. *C*, superimposition of Lyn- (*blue*) and Abl- (2GQG; *green*) Dasatinib-binding sites. Abl residues numbers are in *parentheses*.

r.m.s. deviation of 0.870 Å over 236 Cα atoms. The structural features highlighted above are also present in Abl, accounting for the cross-reactivity of the compound. However, a major difference is observed in the glycine loop between Abl and Lyn, with an 8.2-Å movement of the Cα of Lyn Phe^{258} to the corresponding Abl Tyr^{253} (Fig. 5*C*). Abl Tyr^{253} makes several VDW contacts with the aminothiazole and amide moieties of Dasatinib that are absent in the Lyn complex. The repositioning of the glycine loop also enables the carbonyl oxygen of Abl Gly^{249} to contact the pyrimidine methyl group, which is not seen between the inhibitor and Lyn Gly^{254}. Although the Glycine loop of PTKs is quite flexible, and thus would be expected to be able to accommodate some variety of conformations, it is notable that the Abl glycine loop is in a similar position in the

recently reported structure of the Abl-Nilotinib inhibitor complex (45), and in both cases quite distinct to the location in all 4 Lyn structures reported here (Fig. 4), as well as in other published Src-family PTK structures. Such a distinct structural difference between the Lyn and Abl complexes likely accounts for much of the >10-fold higher affinity of Abl ($IC_{50} < 1$ nM) (42) than Lyn (11 nM, this work) for Dasatinib. The variable hinge residue Ala^{323} (Thr^{319} in Abl) makes VDW contact with the hydroxyethyl-piperazine moiety of Dasatinib through the main-chain carbonyl oxygen. In the Abl complex, Tyr^{320} is within VDW contact distance, which is not seen with Lys^{324} of Lyn. These structural features not only are likely to contribute to different binding affinities for Dasatinib, but, importantly, point the way to further exploitation in the development of future, more specific compounds.

The current study reports the structure of Lyn PTK. Analysis of the binding mode of a series of structurally distinct inhibitors reveals features accounting for their varying specificity to Lyn and other PTKs. Kinase inhibitors are becoming an increasingly important class of chemotherapeutic agents. With the growing recognition of Lyn as a key player in several leukemias as well as solid tumors, these structures will undoubtedly assist with the design of the next generation of clinical therapeutics against Lyn and related molecules.

Acknowledgments—We thank Christina Wang and Cathleena McLaren for assistance with tissue culture. Conflict-of-interest disclosure: The authors declare no competing financial interests.

REFERENCES

1. Xu, W., Doshi, A., Lei, M., Eck, M. J., and Harrison, S. C. (1999) *Mol. Cell* **3,** 629–638
2. Ingley, E. (2008) *Biochim. Biophys. Acta* **1784,** 56–65
3. Pawson, T., and Nash, P. (2000) *Genes Dev.* **14,** 1027–1047
4. Corey, S. J., and Anderson, S. M. (1999) *Blood* **93,** 1–14
5. Rane, S. G., and Reddy, E. P. (2002) *Oncogene* **21,** 3334–3358
6. Parsons, S. J., and Parsons, J. T. (2004) *Oncogene* **23,** 7906–7909
7. Tilbrook, P. A., Ingley, E., Williams, J. H., Hibbs, M. L., and Klinken, S. P. (1997) *EMBO J.* **16,** 1610–1619
8. De Franceschi, L., Fumagalli, L., Olivieri, O., Corrocher, R., Lowell, C. A., and Berton, G. (1997) *J. Clin. Investig.* **99,** 220–227
9. Robinson, D., Chen, H. C., Li, D., Yustein, J. T., He, F., Lin, W. C., Hayman, M. J., and Kung, H. J. (1998) *J. Biochem. Sci.* **5,** 93–100
10. Goldenberg-Furmanov, M., Stein, I., Pikarsky, E., Rubin, H., Kasem, S., Wygoda, M., Weinstein, I., Reuveni, H., and Ben-Sasson, S. A. (2004) *Cancer Res.* **64,** 1058–1066
11. Bates, R. C., Edwards, N. S., Burns, G. F., and Fisher, D. E. (2001) *Cancer Res.* **61,** 5275–5283
12. Tilbrook, P. A., Palmer, G. A., Bittorf, T., McCarthy, D. J., Wright, M. J., Sarna, M. K., Linnekin, D., Cull, V. S., Williams, J. H., Ingley, E., Schneider-Mergener, J., Krystal, G., and Klinken, S. P. (2001) *Cancer Res.* **61,** 2453–2458
13. Ingley, E., McCarthy, D. J., Pore, J. R., Sarna, M. K., Adenan, A. S., Wright, M. J., Erber, W. N., Tilbrook, P. A., and Klinken, S. P. (2005) *Oncogene* **24,** 336–343
14. Linnekin, D., DeBerry, C. S., and Mou, S. (1997) *J. Biol. Chem.* **272,** 27450–27455
15. Lannutti, B. J., and Drachman, J. G. (2004) *Blood* **103,** 3736–3743
16. Ingley, E., Sarna, M. K., Beaumont, J. G., Tilbrook, P. A., Tsai, S., Takemoto, Y., Williams, J. H., and Klinken, S. P. (2000) *J. Biol. Chem.* **275,** 7887–7893
17. Ingley, E., Schneider, J. R., Payne, C. J., McCarthy, D. J., Harder, K. W., Hibbs, M. L., and Klinken, S. P. (2006) *J. Biol. Chem.* **281,** 31920–31929
18. Chin, H., Arai, A., Wakao, H., Kamiyama, R., Miyasaka, N., and Miura, O. (1998) *Blood* **91,** 3734–3745
19. Hibbs, M. L., Tarlinton, D. M., Armes, J., Grail, D., Hodgson, G., Maglitto, R., Stacker, S. A., and Dunn, A. R. (1995) *Cell* **83,** 301–311
20. Harder, K. W., Quilici, C., Naik, E., Inglese, M., Kountouri, N., Turner, A., Zlatic, K., Tarlinton, D. M., and Hibbs, M. L. (2004) *Blood* **104,** 3901–3910
21. Roginskaya, V., Zuo, S., Caudell, E., Nambudiri, G., Kraker, A. J., and Corey, S. J. (1999) *Leukaemia* **13,** 855–861
22. Donato, N. J., Wu, J. Y., Stapley, J., Gallick, G., Lin, H., Arlinghaus, R., and Talpaz, M. (2003) *Blood* **101,** 690–698
23. Golas, J. M., Arndt, K., Etienne, C., Lucas, J., Nardin, D., Gibbons, J., Frost, P., Ye, F., Boschelli, D. H., and Boschelli, F. (2003) *Cancer Res.* **63,** 375–381
24. Warmuth, M., Simon, N., Mitina, O., Mathes, R., Fabbro, D., Manley, P. W., Buchdunger, E., Forster, K., Moarefi, I., and Hallek, M. (2003) *Blood* **101,** 664–672
25. Wilson, M. B., Schreiner, S. J., Choi, H. J., Kamens, J., and Smithgall, T. E. (2002) *Oncogene* **21,** 8075–8088
26. Dos Santos, C., Demur, C., Bardet, V., Prade-Houdellier, N., Payrastre, B., and Recher, C. (2008) *Blood* **111,** 2269–2279
27. Wu, J., Meng, F., Lu, H., Kong, L., Bornmann, W., Peng, Z., Talpaz, M., and Donato, N. J. (2008) *Blood* **111,** 3821–3829
28. Meyn, M. A., III, Wilson, M. B., Abdi, F. A., Fahey, N., Schiavone, A. P., Wu, J., Hochrein, J. M., Engen, J. R., and Smithgall, T. E. (2006) *J. Biol. Chem.* **281,** 30907–30916
29. Pendergast, A. M., Quilliam, L. A., Cripe, L. D., Bassing, C. H., Dai, Z., Li, N., Batzer, A., Rabun, K. M., Der, C. J., Schlessinger, J., and Gishizky, M. L. (1993) *Cell* **75,** 175–185
30. Ptasznik, A., Nakata, Y., Kalota, A., Emerson, S. G., and Gewirtz, A. M. (2004) *Nat. Med.* **10,** 1187–1189
31. Sumitomo, M., Shen, R., Walburg, M., Dai, J., Geng, Y., Navarro, D., Boileau, G., Papandreou, C. N., Giancotti, F. G., Knudsen, B., and Nanus, D. M. (2000) *J. Clin. Investig.* **106,** 1399–1407
32. Druker, B. J., Talpaz, M., Resta, D. J., Peng, B., Buchdunger, E., Ford, J. M., Lydon, N. B., Kantarjian, H., Capdeville, R., Ohno-Jones, S., and Sawyers, C. L. (2001) *N. Engl. J. Med.* **344,** 1031–1037
33. Talpaz, M., Shah, N. P., Kantarjian, H., Donato, N., Nicoll, J., Paquette, R., Cortes, J., O'Brien, S., Nicaise, C., Bleickardt, E., Blackwood-Chirchir, M. A., Iyer, V., Chen, T. T., Huang, F., Decillis, A. P., and Sawyers, C. L. (2006) *N. Engl. J. Med.* **354,** 2531–2541
34. Xu, W., Harrison, S. C., and Eck, M. J. (1997) *Nature* **385,** 595–602
35. Sicheri, F., Moarefi, I., and Kuriyan, J. (1997) *Nature* **385,** 602–609
36. Schindler, T., Sicheri, F., Pico, A., Gazit, A., Levitzki, A., and Kuriyan, J. (1999) *Mol. Cell* **3,** 639–648
37. Yamaguchi, H., and Hendrickson, W. A. (1996) *Nature* **384,** 484–489
38. Zhu, X., Kim, J. L., Newcomb, J. R., Rose, P. E, Stover, D. R., Toledo, L. M., Zhao, H., and Morgenstern, K. A. (1999) *Structure* **7,** 651–661
39. Bringans, S., Eriksen, S., Kendrick, T., Gopalakrishnakone, P., Livk, A., Lock, R., and Lipscombe, R. (2008) *Proteomics* **8,** 1081–1096
40. Ingley, E., Chappell, D., Poon, S. Y., Sarna, M. K., Beaumont, J. G., Williams, J. H., Stillitano, J. P., Tsai, S., Leedman, P. J., Tilbrook, P. A., and Klinken, S. P. (2001) *J. Biol. Chem.* **276,** 43428–43434
41. Tokarski, J. S., Newitt, J. A., Chang, C. Y., Cheng, J. D., Wittekind, M., Kiefer, S. E., Kish, K., Lee, F. Y., Borzillerri, R., Lombardo, L. J., Xie, D., Zhang, Y., and Klei, H. E. (2006) *Cancer Res.* **66,** 5790–5797
42. Lombardo, L. J., Lee, F. Y., Chen, P., Norris, D., Barrish, J. C., Behnia, K., Castaneda, S., Cornelius, L. A., Das, J., Doweyko, A. M., Fairchild, C., Hunt, J. T., Inigo, I., Johnston, K., Kamath, A., Kan, D., Klei, H., Marathe, P., Pang, S., Peterson, R., Pitt, S., Schieven, G. L., Schmidt, R. J., Tokarski, J., Wen, M. L., Wityak, J., and Borzilleri, R. M. (2004) *J. Med. Chem.* **47,** 6658–6661
43. Shah, N. P., Tran, C., Lee, F. Y., Chen, P., Norris, D., and Sawyers, C. L. (2004) *Science* **305,** 399–401
44. Schindler, T., Bornmann, W., Pellicena, P., Miller, W. T., Clarkson, B., and Kuriyan, J. (2000) *Science* **289,** 1938–1942
45. Weisberg, E., Manley, P. W., Breitenstein, W., Brüggen, J., Cowan-Jacob, S. W., Ray, A., Huntly, B., Fabbro, D., Fendrich, G., Hall-Meyers, E., Kung, A. L., Mestan, J., Daley, G. Q., Callahan, L., Catley, L., Cavazza, C., Azam, M., Neuberg, D., Wright, R. D., Gilliland, D. G., and Griffin, J. D. (2005) *Cancer Cell* **7,** 129–141

Crystal Structures of the Lyn Protein Tyrosine Kinase Domain in Its Apo- and Inhibitor-bound State

Neal K. Williams, Isabelle S. Lucet, S. Peter Klinken, Evan Ingley and Jamie Rossjohn

J. Biol. Chem. 2009, 284:284-291.
doi: 10.1074/jbc.M807850200 originally published online November 4, 2008
